A Novel Composited Electromagnetic Linear Actuator

Subjects: Engineering, Mechanical
Contributor: Xinyu Fan

Electromagnetic linear actuators, as key executive components, have a vital impact on the performance of fully flexible variable valve trains. The research results show that the maximum starting force of the composited electromagnetic linear actuator (CELA) with the end-passive self-holding ability is 574.92 N while the holding force can approach 229.25 N. Moreover, the CELA is proven to have excellent dynamic characteristics and control precision under different motion modes and to have an improved adaptability to the complex working conditions of internal combustion engines.

Keywords: composited electromagnetic linear actuator ; internal combustion engine

1. Introduction

As the mainstream driving unit of valve trains, the moving iron electromagnetic linear actuator (MIELA) has the advantages of compact structure and high force density [1], but its single electric excitation type will lead to high energy consumption. The American company Engineering Matters, and Waindok, Yang and Professor Li Xinghu's team proposed hybrid excitation schemes with better driving efficiency and considerable, end-passive self-holding capability [2][3][4][5][6]. However, the inherent nonlinear output driving force of MIELA limited the dynamic performance and control accuracy of the mechanism [7]. As with MIELA, the moving magnetic type was also based on the principle of minimum reluctance in the magnetic circuit. The German company Compact Dynamic [8] and Professor Mercorelli's team [9] proposed a variable valve train scheme based on moving magnetic actuator. However, for the reason that its mover was a permanent magnet, the magnetic field changed obviously in the working process, which increased the difficulty of control.

In recent years, the conventional moving coil electromagnetic linear actuator (MCELA) has attracted extensive attention. The working magnetic field of MCELA is generated by the permanent magnet, and the distribution does not change significantly. This kind of actuator has linear output force, fast response and good control performance. However, MCELA has a low force density, and its dynamic performance needs to be improved when facing high-pressure exhaust gas in the cylinder of internal combustion engines [10][11], and it also lacks end-passive self-holding capacity, which will lead to increased energy consumption.

2. System Structure Design

Figure 1 shows the structure of the composited augmentation-type electromagnetic linear actuator, which is mainly composed of two parts: MCELA and MIELA. They are connected in series, and are fixed with each other through the connecting baffle. Their movers are rigidly connected by mover connecting rod. Two compression springs are fixed in a constant compression state.

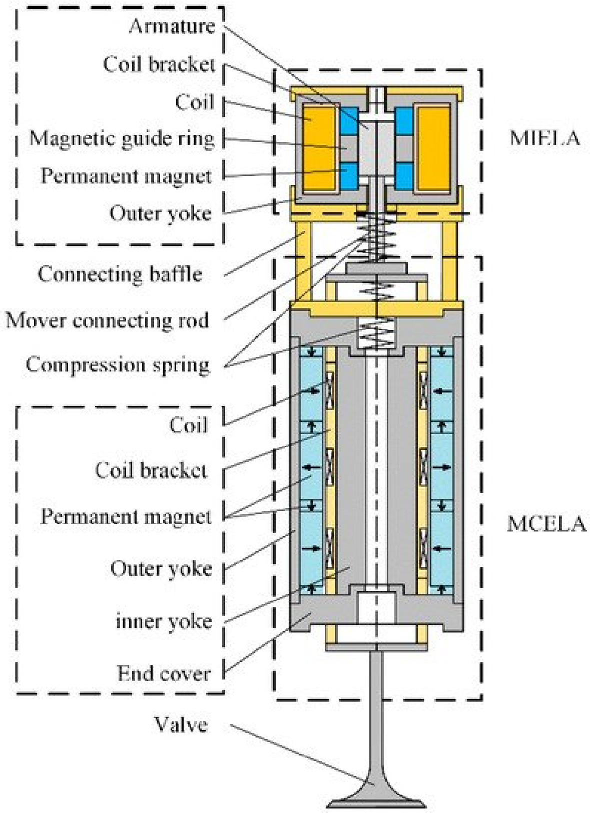

Figure 1. Structure of CELA.

MCELA is the main driving component whose coil bracket is directly connected with the valve and the valve motion control is realized by controlling the coil current. By adopting the Halbach array [12][13] in the internal magnetic field to strengthen the air gap magnetic field strength, MCELA has the characteristics of linear output force and good control performance.

MIElA is an auxiliary driving component based on the principle of minimum reluctance, and it is connected with the coil bracket of MCELA to follow its movement. In addition, MIELA has end-passive self-holding capacity.

2.1. The MCELA

The MCELA is composed of an inner and outer yoke, a coil, a coil bracket, an end cover and a permanent magnet, as shown in **Figure 1**.

The working magnetic field of the MCELA is generated by the permanent magnet, which is divided into a long permanent magnet (radial magnetization) and a short permanent magnet (axial magnetization), and the magnetic flux is the superposition of the magnetic flux generated by the long permanent magnet and the short permanent magnet. The working air gap is a cylinder with an inner diameter of r_1 and an outer diameter of r_2 . The coil moves up and down in the working air gap, which will produce an axial Lorentz force F through the magnetic field when the current I is applied.

By neglecting the leakage flux [14], the corresponding equivalent magnetic circuit can be simplified as shown in **Figure 2**. The figure illustrates the location of the magnetic flux ϕ_l of the long permanent magnet and the magnetic flux ϕ_s of the short permanent magnet in the air gap, where the arrow indicates the direction of the magnetic flux.

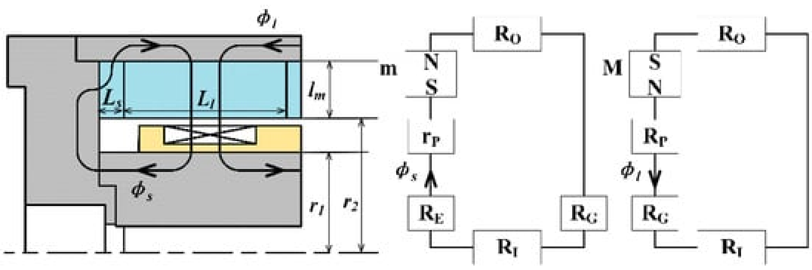

Figure 2. Magnetic Circuit of MCELA.

2.2. The MIELA

MIELA is mainly composed of an armature, an outer yoke, a magnetic guide ring, a coil bracket and a coil, as shown in **Figure 3**.

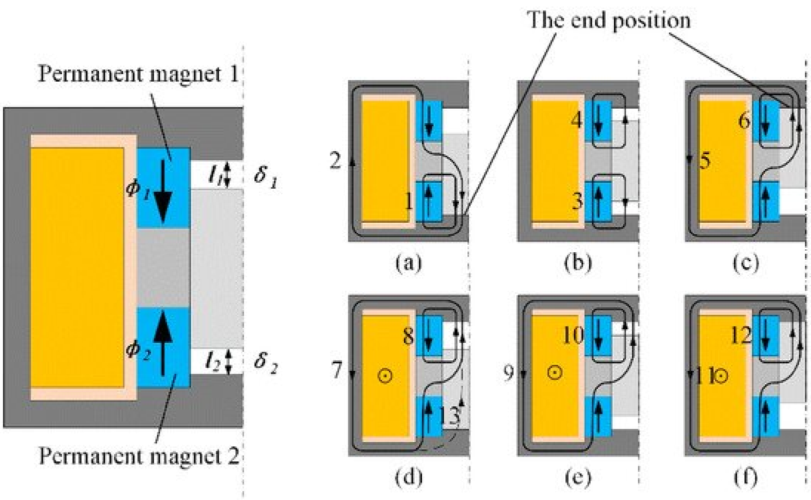

Figure 3. Structure and magnetic circuit analysis diagram of MIELA.

The representative stroke position, two ends and the middle are given as examples in **Figure 3**. For the convenience of description and distinction, the lower permanent magnet is called permanent magnet 1, and the upper permanent magnet is called permanent magnet 2. The magnetization direction of the permanent magnet is also marked in **Figure 3**. When the mover armature is at the beginning and end of the stroke, it is close to the outer yoke, which is called the end position.

3. Three-Dimensional Finite Element Simulation

Three-dimensional finite element (FE) models of MIELA and MCELA were established in the electromagnetic analysis software JMAG to calculate the magnetic field distribution of the actuator.

3.1. MCELA

The finite element model of MCELA is shown in **Figure 4**. In this figure, the coil is in the middle of the stroke, and the arrow indicates the magnetization direction of the permanent magnet. A Halbach array is adopted in the permanent magnet arrangement, which effectively enhances the magnetic flux density on the side of the working air gap. The permanent magnet is made of NdFeB with good performance, and the end cover and inner and outer yoke are made of 1008 steel with strong magnetic conductivity. The coil bracket adopts light-weight, high-strength engineering plastics, which reduces the mass of the movers and reduces the impact on response speed, thus ensuring the strength and life of the actuator.

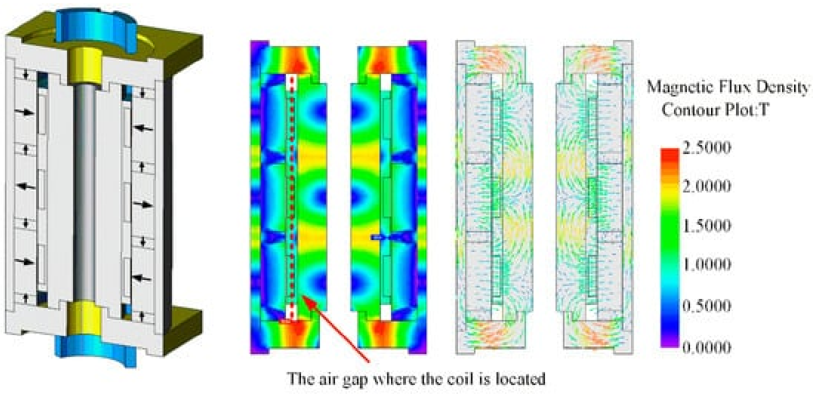

Figure 4. Magnetic flux density cloud and magnetic flux density vector plots of MCELA.

The magnetic field distribution of MCELA is shown in **Figure 4**. It can be seen that the magnetic flux distribution is denser and more uniform in the coil, the magnetic flux density is larger in the upper and lower end covers, and the inner and outer yokes are parallel to the axial magnetized permanent magnet.

The magnetic flux density distribution curve at the air gap is shown in **Figure 5**. Compared with the common array, Halbach array has higher magnetic flux density, and the air gap magnetic flux density curve shows a flat peak within the coil motion range. Within this range, the magnetic flux density is relatively uniform, with smooth force characteristics and good control performance.

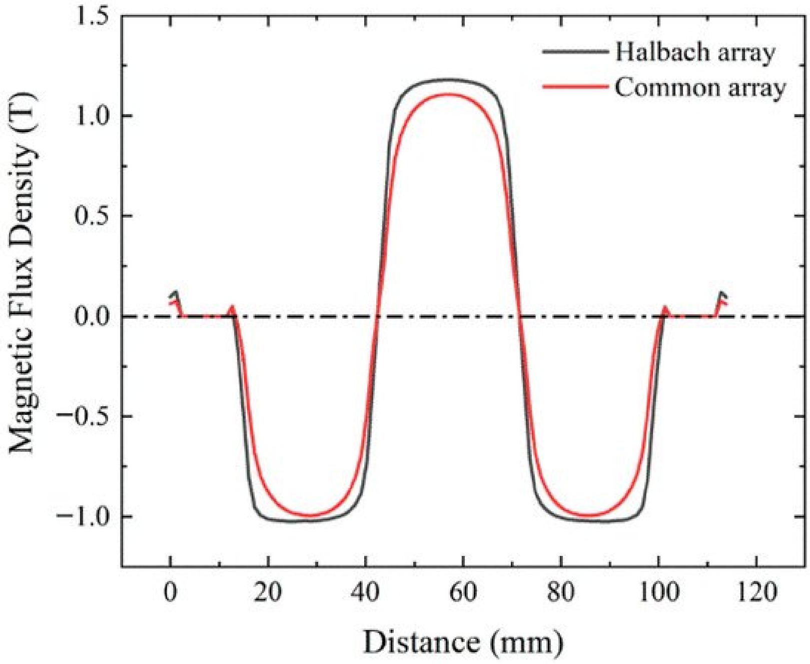

Figure 5. Magnetic flux density distribution curve.

3.2. MIELA

The finite element model of MIELA, with a stroke of 8mm, is shown in **Figure 6**. The armature, outer yoke and magnetic guide ring in the model are made of 1008 steel with strong magnetic conductivity and low cost, and the permanent magnet is made of NdFeB. The coil framework is made of lightweight and high-strength engineering plastics. Encryption was carried out on the meshes of the parts with dramatic magnetic field changes.

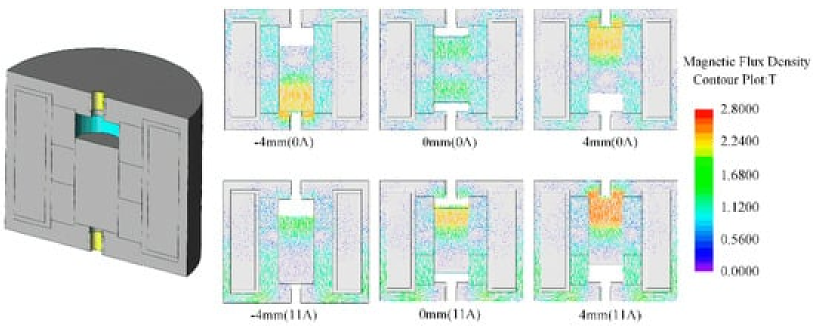

Figure 6. Structure and magnetic flux density vector plots of MIELA.

Figure 6 also shows the electromagnetic field distribution of the armature in different positions under the passive and active states obtained by simulation of the finite element model. It can be seen that the simulation results are consistent with the results of the previous theoretical analysis. The magnetic field changes sharply at the armature, the outer yoke seating position and the magnetic guide ring.

3.3. CELA

CELA is composed of the above two main components MCELA (the main driving component) and MIELA (the auxiliary driving component). The movers between MCELA and MIELA are rigidly connected, so their forces can be coupled directly. There are two symmetrical springs whose stiffness coefficient is 9.8 N/mm between them, and the precompression is 0.4 mm. The steady-state force characteristics of CELA can be obtained directly by combining them. The composite structure of CELA can take into account the performance advantages of MCELA and MIELA, with high starting force and end-passive self-holding force. The specific force characteristics are shown in **Figure 7**.

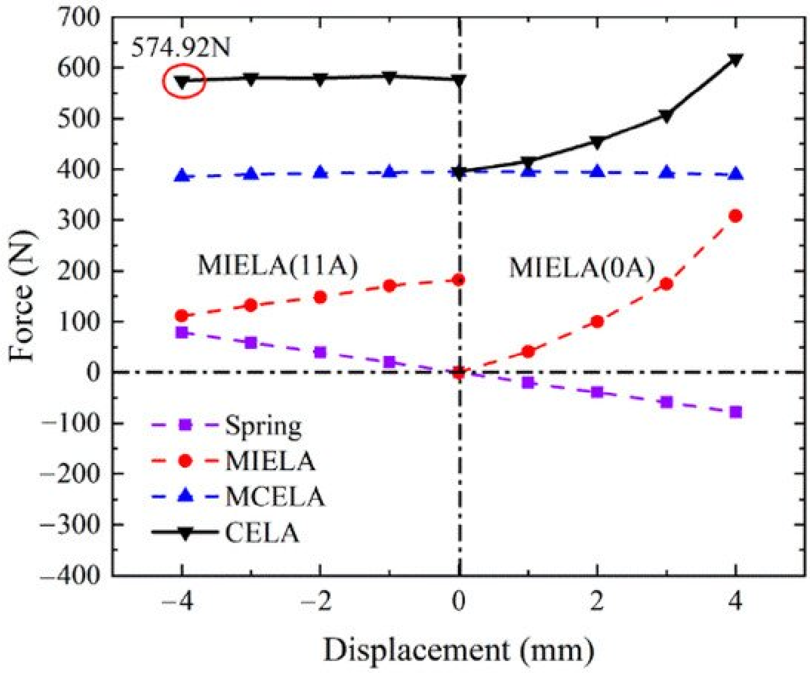

Figure 7. Steady state force–displacement characteristic simulation curve of CELA.

4. Conclusions

A new structural scheme of a composited electromagnetic linear actuator (CELA), which combines the performance advantages of MCELA and MIELA, is proposed. The magnetic field distribution and force characteristics are analyzed through theoretical analysis and simulation analysis, and the multi-mode coordinated motion control strategy is established. An experimental platform was built to verify the steady and dynamic characteristics of CELA, indicating that the design scheme is feasible.

- In CELA, MCELA (which has linear output force and good control performance) is the main driving part. As the auxiliary driving component, MIELA provides end-holding force and selective driving power.
- A multi-mode motion coordination control strategy is established. When the load is large, the two driving parts are energized, and the starting force can be as high as 574.92 N. When the load is small, MCELA is energized alone, and MIELA moves with it to reduce the power consumption of the system.
- At the end of the stroke, CELA has a passive holding force of 229.25 N, which means that additional current is no longer required to counter the disturbance of the gas load during the on/off phase of holding. Thus, it can effectively reduce energy consumption.
- Under different motion modes, CELA can achieve continuous adjustable duration and maximum lift, and has good dynamic characteristics. At the same time, the steady-state error can be kept within ±0.02 mm, with high control accuracy.

References

1. Tan, C.; Ge, W.; Fan, X.; Lu, J.; Li, B.; Sun, B. Bi-stable actuator measurement method based on voice coil motor. Sens. Actuators A Phys. 2019, 285, 59–66.
2. Cope, D.; Wright, A.; Corcoran, C.J.; Pasch, K.; Fischer, D. Fully Flexible Electromagnetic Valve Actuator: Design, Modeling, and Measurements; SAE Intenational: Pittsburgh, PA, USA, 2008.
3. Waindok, A.; Tomczuk, B.; Koteras, D. Modeling of Magnetic Field and Transients in a Novel Permanent Magnet Valve Actuator. Sensors 2020, 20, 2709.
4. Yang, Y.-P.; Liu, J.-J.; Ye, D.-H.; Chen, Y.-R.; Lu, P.-H. Multiobjective Optimal Design and Soft Landing Control of an Electromagnetic Valve Actuator for a Camless Engine. IEEE/ASME Trans. Mechatron. 2012, 18, 963–972.
5. Aslam, J.; Li, X.-H.; Janjua, F.K. Design of a hybrid magnetomotive force electromechanical valve actuator. Front. Inf. Technol. Electron. Eng. 2017, 18, 1635–1643.

6. Tan, C.; Li, B.; Ge, W. Thermal quantitative analysis and design method of bi-stable permanent magnet actuators based on multiphysics methodology. IEEE Trans. Ind. Electron. 2019, 67, 7727–7735.
7. Shao, D.; Sichuan, X.; Du, A. Research on a New Electromagnetic Valve Actuator Based on Voice Coil Motor for Automobile Engines; SAE MOBILUS: Pittsburgh, PA, USA, 2017.
8. Hoffman, B. Fully Variable Valve actuation with electromagnetic Linear Motor. SIA Conf. Var. Valve Actuation 2006, 30, 1–8.
9. Mercorelli, P. A Two-Stage Sliding-Mode High-Gain Observer to Reduce Uncertainties and Disturbances Effects for Sensorless Control in Automotive Applications. IEEE Trans. Ind. Electron. 2015, 62, 5929–5940.
10. Schernus, C.; Van Der Staay, F.; Janssen, H.; Neumeister, J.; Vogt, B.; Donce, L.; Estlimbaum, I.; Nicole, E.; Maerky, C. Modeling of Exhaust Valve Opening in a Camless Engine; SAE International: Pittsburgh, PA, USA, 2002.
11. Fan, X.; Yin, J.; Su, S.; Pang, H.; Song, Y. Loss analysis of electromagnetic valve train under different service conditions. Int. J. Appl. Electromagn. Mech. 2021, 66, 461–473.
12. Li, Z.; Wu, Q.; Liu, B.; Gong, Z. Optimal Design of Magneto-Force-Thermal Parameters for Electromagnetic Actuators with Halbach Array. Actuators 2021, 10, 231.
13. Liu, L.; Chang, S. Improvement of valve seating performance of engine’s electromagnetic valvetrain. Mechatronics 2011, 21, 1234–1238.
14. Kim, J.; Joo, S.; Hahn, S.; Hong, J.; Kang, D.; Koo, D. Static Characteristics of Linear BLDC Motor Using Equivalent Magnetic Circuit and Finite Element Method. IEEE Trans. Magn. 2004, 40, 742–745.